Poly-(pentaerythritol adipate)-co-(poly ethylene glycol) Elastomers for the Sustained Release of Paclitaxel

Lucila Navarro,[1] Roque J. Minari,[1] Natalia Ceaglio,[2] Marianela Masin,[2] Santiago E. Vaillard[1]

[1]Instituto de Desarrollo Tecnológico para la Industria Química (INTEC), CCT-Santa Fe, CONICET-UNL, Colectora Ruta Nacional 168, Km 1, Paraje EL Pozo, Santa Fe 3000, Argentina
[2]Universidad Nacional del Litoral (UNL), CONICET, Facultad de Bioquímica y Ciencias Biológicas, Laboratorio de Cultivos Celulares, Edificio FBCB, Ciudad Universitaria UNL, C.C. 24, (S3000ZAA), Santa Fe, Argentina
Correspondence to: S. E. Vaillard (E-mail: svaillard@intec.unl.edu.ar)

Received 13 February 2018; accepted 7 March 2018; published online 00 Month 2018
DOI: 10.1002/pola.28999

ABSTRACT: Over the past 10 years poly-(polyol alkanoate)s elastomers have intensively been investigated due to their extraordinary potential for soft tissue engineering applications. In this work, a family of novel hyperbranched elastomers based on pentaerythritol and adipic acid, modified with PEG of 200 and 400 Da, is synthesized. The polymers are obtained by a simple 2 steps thermal process that avoids the use of toxic catalysts. Noteworthy, elastomers properties can be finely tuned by adjusting the molar ratio of monomers and curing conditions. The elastomers, which are fully characterized by standard methods, show excellent results in the *in vitro* controlled release of Paclitaxel. Cell culture assays indicate that all materials are able to inhibit lung cancer cell proliferation and that the release of Paclitaxel reduce cancer cell viability, indicating that the elastomers prepared hereby are good candidates for their use as eluting systems in long term cancer treatment. © 2018 Wiley Periodicals, Inc. J. Polym. Sci., Part A: Polym. Chem. **2018**, *00*, 000–000

KEYWORDS: branched; controlled release; drug delivery systems; elastomers; films; hyperbranched polymers; polycondensation

INTRODUCTION Over the last few years, biodegradable elastomers have been the focus of intense research due to their extraordinary potential for various biomedical applications. The fact that the structure and nature of the elastomers can be tuned to finely mimic predefined mechanical properties, early stimulated the evaluation of these innovative biomaterials for soft tissue engineering applications. Nowadays it is widely accepted that for successful biomedical application, bio-elastomers should match the mechanical properties of the host tissue, among various other stringent requirements.[1] Moreover, biodegradable elastomers are widely recognized as interesting alternatives to traditional poly-(lactic-co-glycolic acid) (PLGA) and related thermoplastics, such as poly-(glycolic acid) (PGA) and poly-(lactic acid) (PLA), as they can support the mechanical properties of the host tissue, but without causing irritation in the implantation site.[2–4] Among the various bio-degradable elastomers that have been reported recently,[5] most of the attention have been centered on polyurethanes,[6–8] poly-(polyol alkanoates),[9] including poly-(polyol adipate)s,[10,11] poly-(polyol sebacate)s,[12–15] such as poly-(glycerol-sebacate) and poly-(diol citrate)s.[16–22] All these materials showed good potential for their application in biomedical devices and implants.

Various hyperbranched elastomers based on sebacic acid and carbohydrates have been developed over the last 10 years, such as poly-(xylitol sebacate),[23,24] poly-(mannitol sebacate),[25] poly-(sorbitol sebacate),[15] and poly-(erythritol sebacate),[12,25] which appear to be promising materials for numerous tissue engineering applications. However, the use of star-shape polyols as branched monomers, like pentaerythritol, have been studied only to a limited extent, and most of the attention have been focused in their syntheses and structure characterization.[26]

Despite these materials showed excellent elastomeric properties, their use for drug delivery systems have barely been investigated. It has been demonstrated that polymeric drug-eluting systems can be used to improve the therapeutic efficacy of anti-tumor drugs, like Paclitaxel (PTX).[27,28] However, the preparation of these systems is usually very complex, requiring numerous synthetic steps, such as the addition of cross-linking agents and catalytic reactions using organometallic compounds, which could compromise their biocompatibility.[29,30] Additionally, many of these polymeric release systems show pronounced initial burst drug release phases during the first days, which reduce long-term efficacy.[31]

Achieving complete coverage and drug diffusion across the whole tissue remains, still nowadays, as a major challenge for controlled drug release technology. Some of the strategies that have been developed to reach acceptable tissue coverage include the use of thermoplastic films, the coating of the tissue with polymerizable gels and the application of microparticles using aerosol techniques. However, other issues, like the lack of controlled release and/or mechanical stability, often undermines the utility of these strategies.[32]

Low molecular weight polyethylene glycol (PEG) has been classified as a potent cancer chemo-protective agent.[33–35] It has been suggested that PEG can prevent tumor growth by two different mechanisms. Firstly, cytostatic effects were observed on two human colonic adenocarcinoma lines, by blocking the cell cycle in G_0/G_1 phase, induced by the increase on the osmotic pressure.[36] In addition, a cytotoxic effect, caused by the increase in the levels of Reactive Oxygen Species (ROSs), was also informed. This last hypothesis was recently confirmed by Liu et al. on both Human Cervical cancer cells (HeLa) and on mouse fibroblasts (L929), which exhibited up to 400% increase on ROSs levels, compared to the controls, when cultures were exposed to high concentrations of PEG 200.[37] Given these chemoprotective properties of PEG, we decided to include these monomers in the new materials, which should, in principle, help to increase the long term efficiency of PTX.

In this work, we have prepared novel poly-(pentaerythritol adipate) and poly-(pentaerythritol adipate)-co-(poly ethylene glycol) elastomers aimed for site-specific delivery of PTX on cancerous soft tissue. The on-site release of the anti-cancer drug would prevent the toxic systemic effects obtained on traditional intravenous chemotherapy, at the time that would help to prevent recurrence. The elastomers were obtained by a 2-steps thermal procedure, which does not require the use of toxic organometallic catalyst, or cross-linking reagents. The set of new materials, which showed tunable properties, were fully characterized by different methods and techniques. In addition, the release profile of PTX from the polymeric matrices proved to be sustained, without showing pronounced burst release phases, supporting the potential of the new polymer matrixes. *In vitro* anti-proliferative assays performed on human lung cancer cells showed that the material alone had a cytostatic effect. Moreover, the addition of PTX has cytotoxic effect, reducing cancer cell viability. These results suggest that the drug eluting elastomers could be useful for controlling tumor growth by long term local release of PTX.

EXPERIMENTAL

Materials and Methods

Pentaerythritol, adipic acid, PEG of molecular weights of 200 Da and 400Da, $CDCl_3$, DMSO-d_6, ethanol, methanol, and ACN are all commercially available and were used as received from the suppliers.

DMF and DMSO were distilled under vacuum and stored over molecular sieves (4 Å). THF was distilled from KOH and stored over molecular sieves (4 Å). PTX (98%) was kindly provided by Bioprofarma (Buenos Aires, Argentina).

Prepolymer Synthesis and Characterization

The synthesis of prepolymer **1** is representative: 8.20 g of pentaerythritol (60 mmol) and 8.76 g of adipic acid (60 mmol) were added to a 100 mL round-bottomed flask equipped with a Dean Stark trap and a reflux condenser. The reaction mixture was stirred at 160 °C under N_2 atmosphere for 1 h. Then, the reaction mixture was heated for 2 h at the same temperature under high vacuum (3 mmHg) and allowed to reach room temperature. Prepolymers **2** and **3** were obtained by adding specific amounts of PEG 200 and PEG 400 to the bulk reaction mixtures previous to the beginning of heating.

Mass average molar mass (M_w), and Number average molar mass (M_n) were determined by Gel permeation chromatography analyses (GPC) using a Waters 1525 instrument equipped with a refractive index detector (Waters 2414) and a SHODEX KD-802.5 column. Prepolymer solutions (1 wt %) were prepared in DMF. The elution rate was 1 mL/min (DMF) and poly-styrene standards were used for the molecular weight calibration curve.

^{1}H-NMR spectra were obtained with a Bruker Avance II, 300 MHZ spectrometer using DMSO-d_6 or $CDCl_3$ containing 5% DMSO. The spectra were referenced to residual solvent signals (2.53 and 7.28 ppm for DMSO-d_6 or $CDCl_3$ respectively). Signal suppression experiments using $CDCl_3$ containing 5% DMSO were performed using WATERSUP pulse program with o1p at 2.53 ppm.

Prepolymer **1**: ^{1}H-NMR (300 MHz, DMSO-d_6): 1.50 (C*H2*, adipic acid); 2.08–2.31 (—O—C(O) —CH_2, adipic acid); 3.91–4.00 (—O—CH_2, pentaerythritol).

Prepolymer **2a-c** and **3a-c**: ^{1}H-NMR (300 MHz, DMSO-d_6): 1.50 (C*H2*, adipic acid); 2.08–2.31 (—O—C(O) —CH_2, adipic acid); 3.38–3.42 (CH_2—CH_2—OC(O), PEG); 3.50 (O—CH_2—CH_2—O, PEG); 23.91–4.00 (—O—CH_2, pentaerythritol).

Fourier transform infrared (FTIR) spectra were obtained with a Shimadzu 8201 PC apparatus.

Film Preparation and Characterization

All prepolymers were dissolved in DMSO, and the solutions were cast onto glass slides previously treated with a thin layer of alginate. The solvent was allowed to evaporate on a heating plate for 5 min, and then, the glasses were heated at 120 °C in an oven from 2 to 5 days. After heating, the glass slides were allowed to reach room temperature and rinsed with water to delaminate the elastomeric films.

To eliminate un-reacted monomers, the films were washed in increasing concentrations of ethanol-water solution mixtures (50, 60, and 80%) for 2 h and with 100% ethanol overnight.

Gel Content

In order of evaluating the cross-linking efficiency, the gel content (%) of elastomers was determined by a Soxhlet extraction with ethanol as solvent. Samples were extracted for 24 h and then allowed to dry at room temperature for 48 h. Gel content (%) was determined by weighting the films before and after the extraction process as follows (eq 1):

$$\text{Gel Content}\,[\%] = \frac{mf}{mi}\text{x } 100 \tag{1}$$

Where, m_i and m_f are the initial and final mass of the elastomeric film.

Static Contact Angle

Static contact angle (θ) measurements were performed with a goniometric homemade device. θ values were determined using the sessile drop method with distilled water. Images were processed with the LBADSA software, based on the fitting of the Young-Laplace equation, and the reported average θ was obtained from five measurements of each sample.[38]

Thermal Properties

Thermal gravimetric analyses (TGA) were done under air from room temperature to 600 °C, at a heating rate of 10 °C/min, using a Mettler-Toledo TGA/SDTA851e/LF/1100 apparatus. Differential scanning calorimetry (DSC) studies were made using DSCQ2000, TA instrument and with heating and cooling rates of 10 °C/min, between −90 °C and 150 °C under nitrogen.

Swelling Index

Swelling indexes by hydration were measured by immersing elastomeric disc samples (8 mm × 1 mm thick) in a PBS buffer pH 7.4. Samples were withdrawn at different times, and the excess of water was carefully removed from the surface with absorbent paper and then weighed. The swelling index was calculated as indicated in eq 2:

$$\text{Swelling Index}\,[\%] = \frac{Ws - Wo}{Wo} \times 100 \tag{2}$$

Where, W_s is the wet mass and W_o is the initial mass.

Swelling indexes were also measured using organic solvents (DCM, ethanol, DMSO, acetonitrile and THF).

Tensile Test

For tensile properties, dog bone-shaped specimens were cut from the polymeric films. Tensile assays were performed at room temperature with an Instron 3344 universal testing machine equipped with a 100 N load cell. The elongation rates were maintained at 10 mm/min and all samples were elongated to failure. Young's moduli (E) were calculated from the slope of the elastic stress-strain curves of three samples.

Cross-linking densities (n) were estimated based on the theory of rubber elasticity using eq 3:

$$\eta = \frac{YM}{3RT} \tag{3}$$

where n is the number of network chain segments per unit volume (mol/m^3), E is the Young's modulus (Pa), R is the universal gas constant (8.3144 J/mol K), and T is the absolute temperature (295 K).

In Vitro Degradation

In vitro degradation studies were performed in PBS buffer pH 7.4 at 37 °C. Elastomer disks (8 mm × 1 mm) were immersed in PBS buffer at 37 °C for different times, after which the samples were withdrawn, washed with water and left to dry for 48 h in oven (50 °C). Mass losses were calculated by weighting the disks before and after the experiment as follows (eq 4):

$$\text{Mass Loss}\,[\%] = \frac{(Mo - MP)}{Mo} \times 100 \tag{4}$$

Where, MP is the dry mass at period of time p and M_o is the initial mass.

PTX Release

Discs of 8 mm of diameter were cut from elastomeric films and immersed in a PTX solution of 20 mg/mL in DCM or THF. The samples were incubated for 24 h and then washed with solvent to remove PTX from the material surface. Each sample was left to dry for 24 h in oven at 50 °C. The amount of PTX loaded to the elastomer was calculated according to eq 5.

$$\text{PTXcontent}\,[\%] = \frac{(Md - MP)}{Md} \times 100 \tag{5}$$

Where, M_d is the initial dry mass and MP is the dry mass after incubation in PTX solution.

PBS pH 7.4 with 0.3% sodium dodecyl sulfate (SDS) was used as the release medium to ensure PTX dissolution (solubility: 61.9 ± 1.7 μg/mL). Elastomeric discs were immersed in 3 mL of release buffer under orbital shaking at 37 °C. Samples were taken after different times and replaced with fresh buffer. Sink conditions were maintained throughout the experiment.

PTX content was determined by HPLC using a HICROM Ultrasphere C18, 5 μ, 250 mm × 4.6 mm column and water/MeOH/ACN (25:11:64) as solvent mixture at 1.0 mL/min rate. Samples were previously filtered using a nylon filter of 0.45 μm. A 20 μL injection volume was used and PTX detection was performed at 227 nm. Calibration curve was produced using standard solutions of the following concentration: 0.5, 12.5, 25, 50, and 75 mg/L.

In Vitro Anti-Tumor Activity

A549 lung adenocarcinoma cell line (ATCC®CCL-185™) was chosen as a model to evaluate the anti-proliferative effect of PTX-loaded polymers over cancer cells. Cells were grown in Dulbecco's Modified of Eagle's Medium (DMEM) (Gibco, USA)

TABLE 1 Synthesis and properties of prepolymers 1, 2a-c, and 3a-c

Material[a]	A:PE:PEG[b]	Time (h)[c]	M_W
1	1:1:0	1	68,300
2a	1:0.75:0.25	4	60,600
2b	1:0.50:0.50	9	57,300
2c	1:0.25:0.75	20	70,200
3a	1:0.75:0.25	5	58,600
3b	1:0.50:0.50	17	68,600
3c	1:0.25:0.75	46	68,200

[a] PEG 200 and PEG 400 were used to obtain prepolymers 2 and 3, respectively.
[b] Molar ratio of A: adipic acid, PE: pentaerythritol and PEG: poly (ethylene glycol).
[c] All reactions were performed at 160 °C for the times indicated, followed by 2 h of reaction at the same temperature under high vacuum (3 mmHg), except for material 1, for which the period of time was reduce to 1 h.

supplemented with 10% fetal calf serum (FSC, Gibco) and 2 mM L-glutamine (Gibco), at 37 °C in humidified atmosphere, 95% air and 5% CO_2. Elastomeric films were prepared as aforementioned and cut into 5 mm discs. Half of the discs were loaded with PTX (see previous paragraph) while the rest was left untreated. Polymer discs (untreatead and PTX-loaded) were placed in 96-well plates and exposed to UV light for 30 min to prevent contamination. A549 cells were trypsinized and seeded in 96-well plates at a density of 1×10^4 cells per well over untreated polymers, PTX-loaded polymers and directly over the well (no polymer), either in the absence (viability control) or in the presence of 0.5 μg/mL PTX (death control). Cell viability was assessed by the MTS assay using a chromogenic kit (CellTiter 96TM AQueous Non-Radioactive Cell Proliferation Assay, Promega) after 3, 5, and 7 days of culture. The plates were read at 492 and 690 nm with a microplate reader and the signal intensity was reported as the mean of the absorbance measured in five wells. In addition, images were taken at 100× magnification at the same incubation times.

RESULTS AND DISCUSSION

Synthesis and Characterization of Prepolymers

To avoid the use of potentially toxic metal or organometallic catalysts or cross-linking agents, we decided to explore the preparation of the required elastomers by a two-step strategy. First, a thermal polycondensation reaction should provide low molecular weight prepolymers, which can be converted to the target elastomeric polymers by cross-linking for longer reaction times. Thus, three types of prepolymers were obtained by melt polycondensation reactions, according to the experimental condition presented in Table 1. Prepolymer **1** (Fig. 1) was obtained using 1 molar equivalent of adipic acid and pentaerythritol (prepolymer **1**, Table 1), while prepolymers **2a-c** and **3a-c** (Fig. 1) were obtained by co-polycondensation with PEGs of two different molecular weights (PEG 200 for prepolymers **2** and PEG 400 for prepolymers **3**, **Table** 1). Furthermore, pentaerythritol/PEG molar ratios were modified in order of reaching different cross-linking degrees, which would control the properties of the final elastomeric films. All prepolymers were obtained as yellowish, highly viscose transparent liquids, which were soluble in dimethylformamide (DMF) and dimethylsulfoxide (DMSO), and insoluble in organic solvents of lower polarity, like dichloromethane (DCM), tetrahydrofuran (THF), and chloroform.

Visually, the viscosity appears to decrease as the molecular weight or the molar ratio of PEG increases. For all prepolymers M_w was obtained by GPC using DMF as eluent. These results are summarized in Table 1.

The structures of prepolymers **1**, **2a-c**, and **3a-c** were further characterized by ^{1}H-NMR. The signals of protons corresponding to the repetitive oxy-ethylene unit of PEG-containing polymers (**2** and **3**, —OCH_2CH_2— units), appear at around 3.6–3.4 ppm. In all cases, signals at around 1.5 ppm are assigned to the aliphatic chain protons of adipic acid and signals at around 2.20 to 2.35 ppm should belong to the protons in the α position to the carboxylate groups. In the same fashion, signals in the 3.9–4.1 ppm range could be assigned to —CH_2— of pentaerythritol.

FTIR spectra of **1**, **2a-c**, and **3a-c** are shown in Figure 2(**b**). All spectra show a sharp and strong peak at 1750 cm^{-1} corresponding to carboxylic C═O stretching and a broad signal

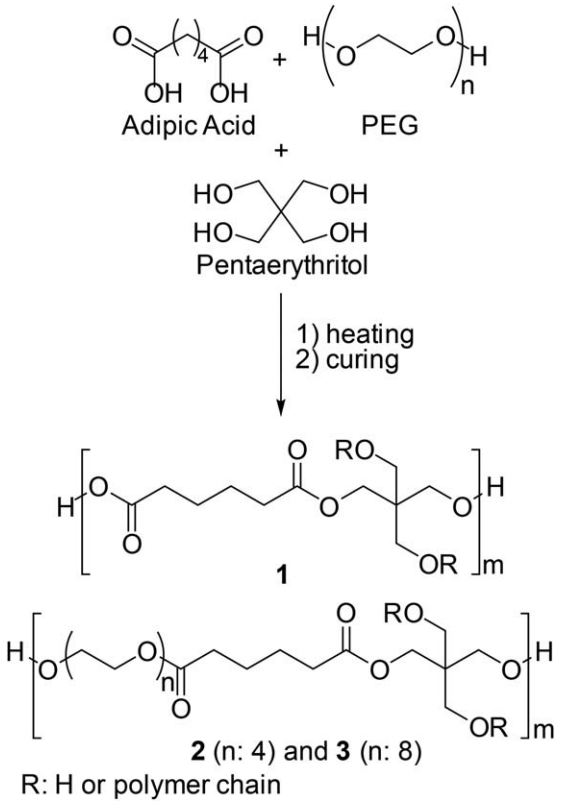

FIGURE 1 Synthesis and structure of prepolymers **1**, **2**, and **3**.

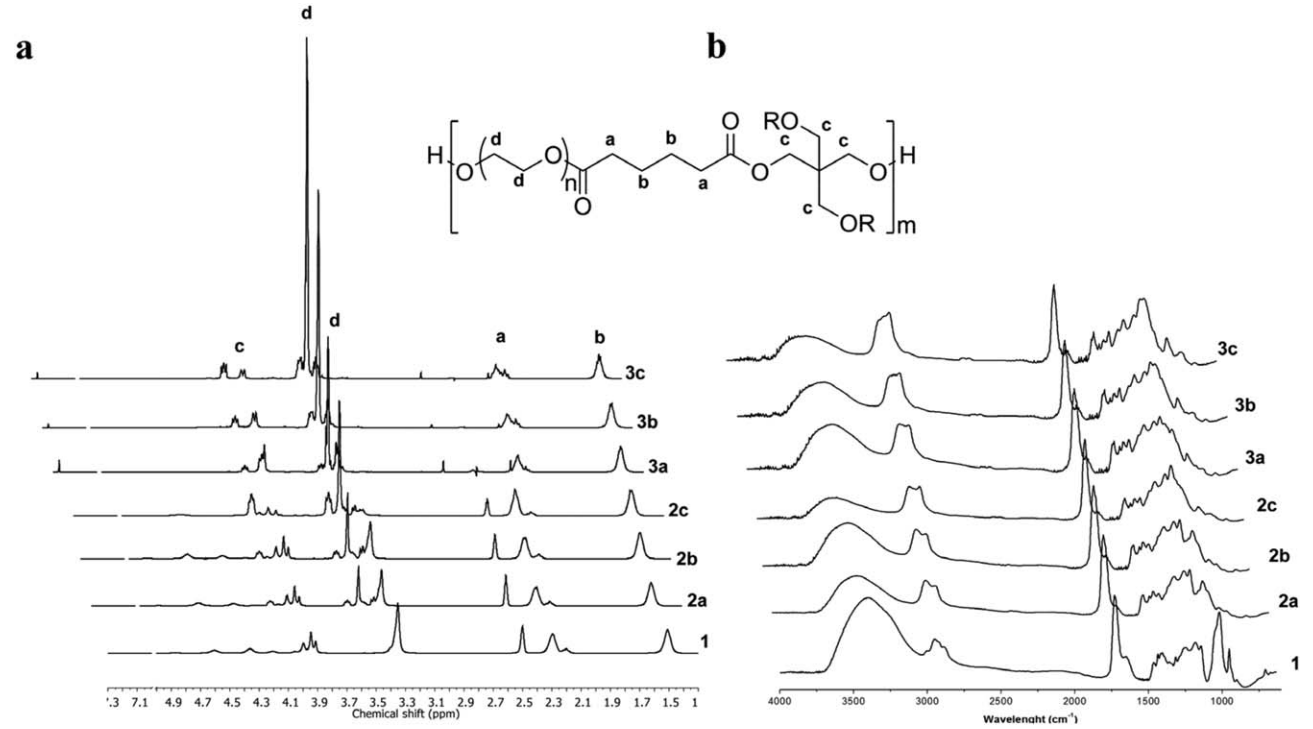

FIGURE 2 ^{1}H-NMR (a) and FTIR (b) spectra of prepolymers **1**, **2a-c**, and **3a-c**.

at approximately 3500 cm^{-1} corresponding to O—H stretching. O—H stretching is more intense in prepolymer **1** given that this prepolymer contains the highest molar ratio of pentaerythritol. Furthermore, typical aliphatic C—H absorption peaks appear at 2670 cm^{-1} on all spectra.

Synthesis and Characterization of Elastomers

All prepolymers were cured (i.e., cross-linked) into elastomeric films by heating in an oven at 120 °C. To control the cross-linking degree, and hence the final mechanical properties of the elastomeric films, two different curing times were used (2 and 5 days).

Gel contents (%) of the elastomeric films were obtained by Soxlhet extraction with ethanol and these results were used as measurement of the cross-linking reaction efficiency (Fig. 3).

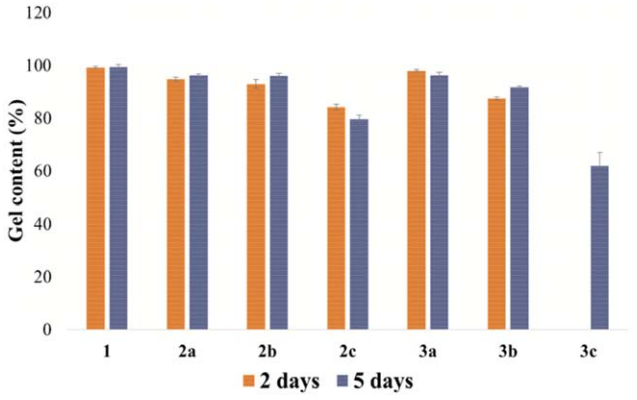

FIGURE 3 Gel content of elastomeric films. [Color figure can be viewed at wileyonlinelibrary.com]

As shown in Figure 3, no significant differences were found for the elastomers cured for 2 and 5 days. In contrast, polymers with highest content of PEG (**2c** and **3c)** rendered the lowest gel content values ($79.54 \pm 1.55\%$ and $61.72 \pm 5.10\%$, respectively, for 5-day-cured polymers). Prepolymer **3c** was not able to provide a solid film after 2 days of curing. Even after 5 days of heating, the gel content remained unacceptably low.

Elastomeric films **1**, **2a-c**, and **3a-b** were further characterized by TGA (Table 2).

TGA thermograms showed two-stage decomposition profiles. At 10% weight loss ($T_{d10\%}$ in Table 2), the elastomers showed a clear tendency: as PEG content, or PEG molecular

TABLE 2 Thermal properties and static contact angle (θ) of elastomers cured for 5 days c

Elastomer	$T_{d10\%}$(°C)	T_d (°C)	T_g (°C)	θ (°)
1	310	430	8.2	76.3 ± 5.3
2a	311	443	−13.0	72.7 ± 1.0
2b	278	436	−23.1	62.3 ± 2.3
2c	272	420	−35.4	65.0 ± 2.9
3a	301	436	−23.0	61.7 ± 2.9
3b	275	426	−34.1	60.4 ± 0.7
3c	225	420	−47.0	NC

weight, increase, temperature decreases. Nevertheless, $T_{d10\%}$(°C) values between 310 °C and 225 °C were registered in all cases (Table 2), which suggest that these elastomeric films are thermally stable and could tolerate the high temperatures required for thermal sterilization. DSC thermograms showed that the glass transition temperatures (T_g) of all polymers were much lower than physiologic temperature, indicating that once the films are placed in the body, the material would adopt a conformational chain of rubbery state. The highest value of T_g was registered for elastomer **1,** as shown in Table 2.

It is clear that as the molar ratio of PEG increases, or as increases the molecular weight of PEG at the same PEG/pentaerythritol content, T_g decreases. With each increment of PEG of 25 molar % with respect to pentaerythritol (Table 1), the T_g decreases, approximately by 10 °C (Table 2). Thus, T_g values for elastomers **2a**, **2b**, and **2c** are −13.0, −23.1, and −35.4 °C, respectively. Accordingly, for PEG/pentaerythritol molar ratio of 0.75/0.25 (elastomers **2c** and **3c**), the increase of the molecular weight of PEG conducted to a decrease of the T_g from −35.4 °C for elastomer **2c** to −47.0 °C for polymer **3c**. Probably, as the length of the PEG chain increases, or as pentaerythritol content decreases, the cross-linking points should be more separated from each other, which would allow the polymer to have higher molecular movement at lower glass transition temperatures. It is also worth to mention that no crystallization or melting temperatures were registered on any elastomer, within the evaluated temperature range. Given that polymer **3c** afforded unacceptably low gel content (Fig. 3), this material was discarded and no further characterization was performed.

The wettability of the polymer surfaces was evaluated based on static contact angle (θ) measurements using distilled water as dispensed drop (Table 2). The results obtained indicated that the most hydrophobic material was polymer **1**, with a value of 76.3 ± 5.3° (Table 2), and that the addition of PEG to the polymer tends to increase the wettability, showing lower values of θ, which agrees with the expected hydrophilic nature of PEG. This result is not surprising, as the increase of hydrophilicity by conjugation to PEG is a well-known and understood phenomenon that have been exploited to increase water solubility of non-polar drugs.[39]

The hydration properties of the materials were studied by mean of the swelling due to water uptake under physiological conditions (PBS buffer, pH 7.4, at 37 °C, Fig. 4), which was monitored periodically.

The evaluation of the effect of curing time revealed that elastomers cured for 5 days showed lower water uptakes than elastomers cured for 2 days. Probably, at longer curing times, the cross-linking degree increases due to the formation of new ester linkages, which ultimately translates in hindered water penetration into the bulk of the polymer, together with decreased swelling capacity and lowered water uptakes. Conversely, the addition of PEG showed an increase of water uptake, this result could be assigned to a higher surface and bulk hydrophilicity of the material and a lower number of cross-linking points, which might allow easier water penetration. It is interesting to note that the water content of the materials (ranging from 17.8 ± 1.6% to 112.5 ± 5.6%, Fig. 4), can easily be tailored by selection of monomer molar ratios, or by modifying the curing conditions.

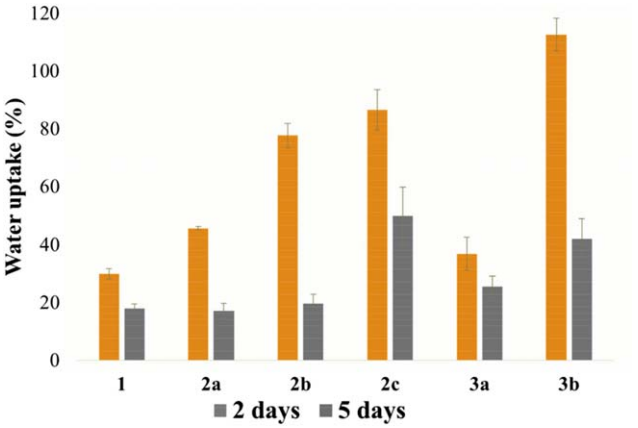

FIGURE 4 Water up take of elastomeric films **1**, **2a-c**, and **3a-b**. [Color figure can be viewed at wileyonlinelibrary.com]

Hydrolytic degradation was evaluated *in vitro* for 5 days-cured films at 37 °C under orbital agitation (Fig. 5).

The slowest degradation rate was observed for material **1**. This result was expected, given that this elastomer has the highest pentaerythritol content, and hence the most cross-linked network, the lowest water uptake and the highest θ. On the contrary, the addition of PEG, or the increase of the molecular weight of PEG, tends to increase the degradation rate. For 30 days of incubation mass losses of 3.8 ± 1.4, 7.8 ± 0.8, 20.3 ± 3.1, and 35.3 ± 0.3% were registered for elastomers **1**, **2a**, **2b**, and **2c**, respectively (Fig. 5). In the same fashion, mass losses for elastomers **3a** and **3b** were 12.5 ± 0.5 and 28.0 ± 1.2%, respectively.

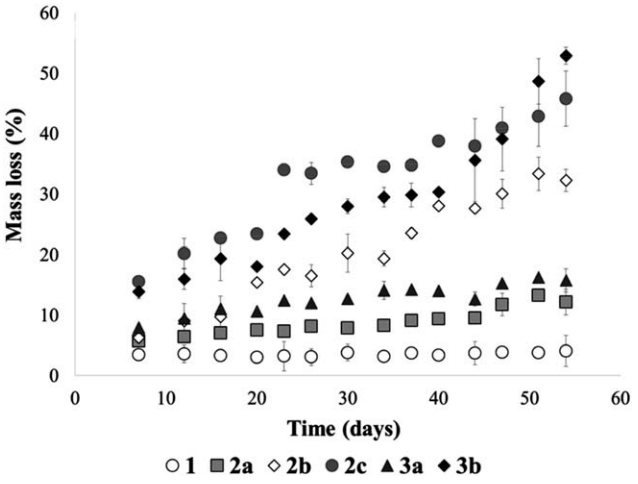

FIGURE 5 Mass losses for hydrolytic degradation of elastomers cured for 5 days.

TABLE 3 Tensile properties of elastomers after 2 and 5 days of curing

	2 Days		5 Days	
Elastomer	E^a	η^b	E	η
1	5.55 ± 021	7.44 ± 0.28	9.21 ± 0.41	12.4 ± 0.34
2a	5.00 ± 0.71	6.75 ± 0.96	8.40 ± 0.71	11.34 ± 0.96
2b	3.90 ± 0.80	5.27 ± 1.15	8.60 ± 0.14	11.62 ± 0.19
2c	1.07 ± 0.09	1.40 ± 0.24	7.25 ± 0.07	9.79 ± 0.10
3a	2.70 ± 0.14	3.65 ± 0.19	5.07 ± 0.38	6.84 ± 0.51
3b	1.04 ± 0.01	1.40 ± 0.02	3.82 ± 0.08	5.09 ± 0.21

[a] MPa.
[b] 10^{-4} (mol/m^3).

Mechanical properties of the elastomers were evaluated through tensile elongation until rupture. Young's modulus (E) was obtained from the slope of the tensile curve and was used to calculate the cross-linking degree (η). These results, which are shown in Table 3, supports the theory that the increase of the molar ratio of PEG, or the increase of PEG molecular weight, might increase the separation of the cross-linking points provided by pentaerythritol, affording more mobility, and lowering the E values. As expected, the materials cured for 5 days showed higher E and η than those cured for 2 days, probably due to the formation of new ester bonds, which would provide more cross-linked elastomeric networks (Table 3).

The fact that not significant differences were found in the gel content of each pair of materials, but yes in the water uptake and mechanical properties, could be related to the high cross-linking degree reached after 2 days of curing. In other words, if the elastomers cured for 2 days already have high cross-linking degrees, the insoluble fraction and gel content will be high, and these materials would present a similar macroscopic behavior than the elastomers cured for 5 days. Despite materials cured for 2 and 5 have days give similar insoluble fraction values, and therefore artificially similar, but still mistaken, cross-linking degrees, the differences observed in the water uptake and E clearly indicates that the polymers cured for 5 days are more cross-linked than materials cured for 2 days.

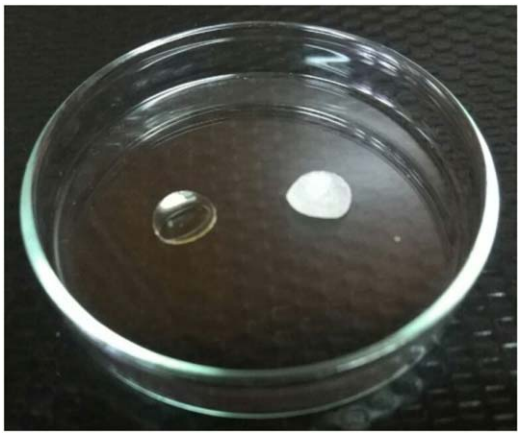

FIGURE 7 Photography **3b** incubated in the release buffer, which has been loaded in THF (left) DCM (right). [Color figure can be viewed at wileyonlinelibrary.com]

Controlled Release of PTX

The use of elastomeric materials as drug eluting systems has only scarcely been reported. For example, Sun and co-workers used poly-(glycerol sebacate) (PGS) for controlled release of anti-cancer drug 5-fluorouracil.[17] The release system was obtained by mixing the drug and prepolymer followed by thermal curing. So, the utility of this method is limited to thermally stable drugs, which must survive unchanged and bio-active to the extreme conditions usually required for the curing processes. To overcome this limitation, we decided to take advantage of the swelling capabilities of the films, which should allow the loading of the drug

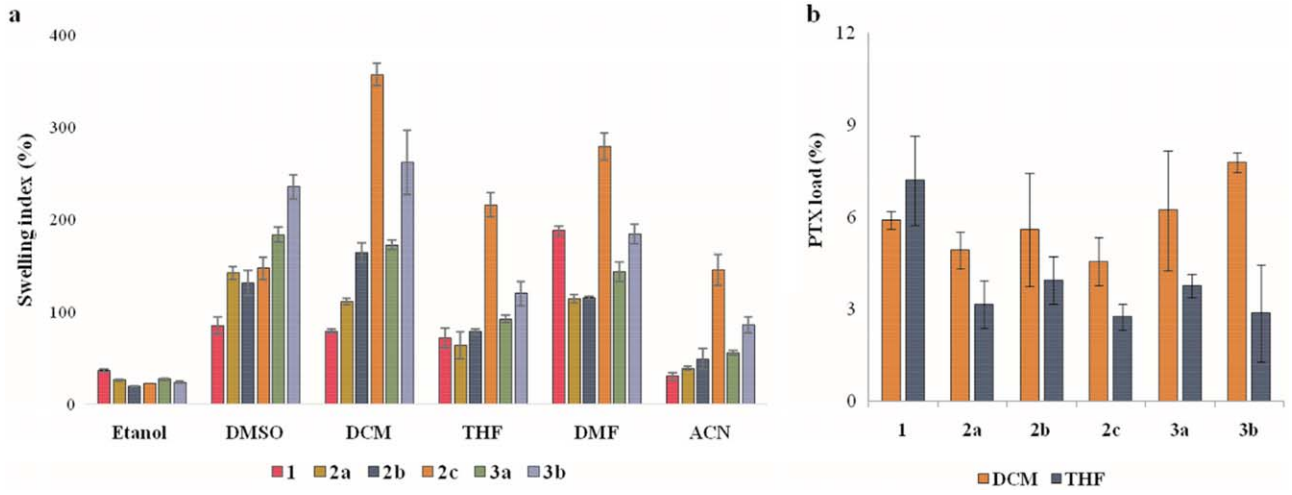

FIGURE 6 (a) Polymer swelling in different organic solvents. (b) Paclitaxel loaded polymer films. [Color figure can be viewed at wileyonlinelibrary.com]

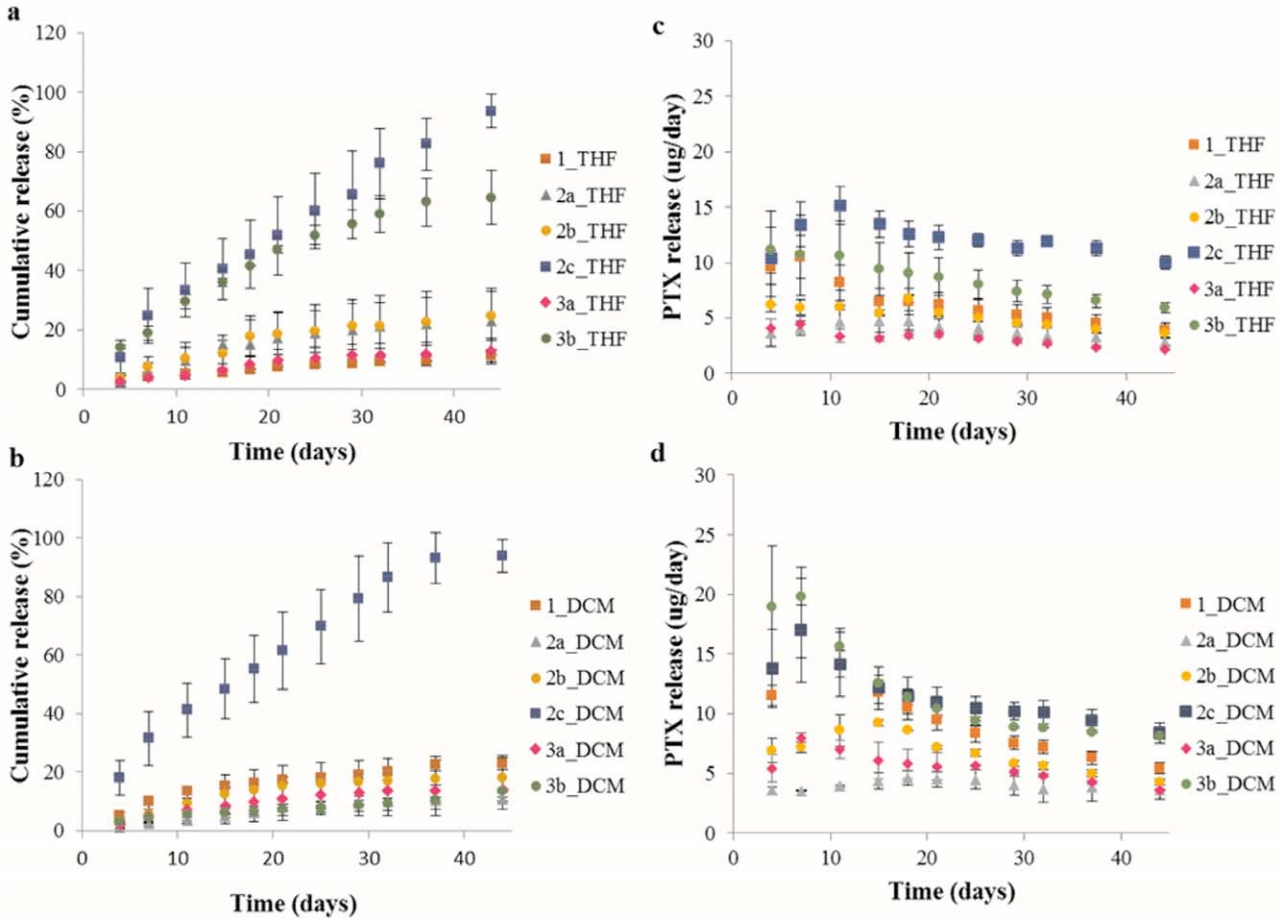

FIGURE 8 (a) PTX cumulative release of elastomeric films loaded in THF. (b) PTX cumulative release of elastomeric films loaded in DCM. (c) PTX release per day of elastomeric films loaded in THF. (d) PTX release per day of elastomeric films loaded in DCM. [Color figure can be viewed at wileyonlinelibrary.com]

in the polymer matrixes, without the need of curing under harsh experimental conditions. To perform the swelling experiments, it was mandatory to choose organic solvents on which PTX was soluble. Ethanol, the most polar solvent evaluated in these studies, showed the lowest swelling indexes, followed by acetonitrile (ACN) [Fig. 6(a)]. Although DMSO

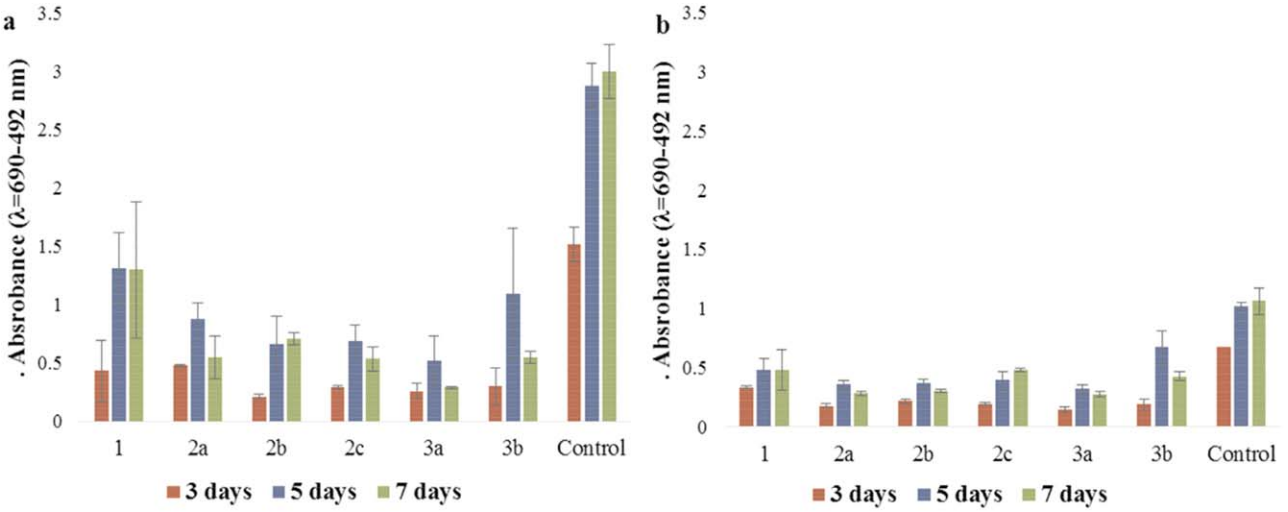

FIGURE 9 *In vitro* cell proliferation assays of A549. (a) Polymers. (b) Polymers loaded with PTX. [Color figure can be viewed at wileyonlinelibrary.com]

and DMF showed higher swelling values, during the weighting of swollen materials we noticed the formation of droplets on the surface of the films, probably of water, and caused by hygroscopic nature of these solvents. Thus, DCM or THF, which have good swelling indexes [Fig. 6(a)], were selected for the drug-loading procedure.

For PTX loading experiments, elastomer discs of 8 mm of diameter and 1 mm of thickness were cut and immersed in a 20 mg/mL solution of PTX using DCM and THF as solvents. Polymer discs were incubated and left to swell for 24 h; then, the films were drawn and washed with solvent to remove PTX from the surface, and finally, left to dry at room temperature for 48 h. The amount of loaded PTX was determined by weighting the discs before and after the swelling process [Fig. 6(b)]. It was not surprising to find that the amounts of loaded PTX were consistently higher using DCM, given that this solvent afforded higher swelling indexes than THF. An exception was elastomer **1**, for which similar drug loadings were found for both solvents [Fig. 6(b)].

With the purpose of obtaining the release profiles, PTX loaded samples were incubated in buffer PBS-0.3% SDS pH 7.4 (37 °C). At predetermined times, samples were taken for quantification of released PTX and the release medium was replaced with fresh buffer. For polymers **2c** and **3b**, loaded with PTX dissolved in DCM, we found that the films turned white and opaque when they were immersed in the release medium (Fig. 7).

This effect was not observed when THF was used to dissolve PTX. DCM is more volatile than THF (vapor pressures for DCM and THF are 475 and 200 hPa, respectively). Thus, we believe that as a consequence of the higher evaporation rate of DCM, the polymer network could not have enough time to relax after loading, generating tension, and leading to the formation micro-fractures throughout the materials. Then, when these materials are immersed in buffer solutions, water would penetrate through the micro-fractures, giving opaque appearance, characteristic of thermoplastic like behaviors, as observed, for example, with poly-(lactic-co-glycolic acid).[40]

The fact that elastomers **2c** and **3b** present the highest swelling indexes in DCM, further support our observation. Despite the unusual behavior of **2c** and **3b** films loaded in DCM, we decided to continue with the release experiments of these two materials, in order of evaluating the appearance of other differences at prolonged times. Figure 8(a,b) shows cumulative PTX release profiles for the films loaded in THF and DCM, respectively. The experiments were conducted for 44 days, time at which polymer **2c** was completely degraded. A sustained release was observed for all polymers loaded in THF and the release rate could easily be adjusted by selecting the right material. As can be seen in Figure 8(a), the fastest release was obtained for polymer **2c** and the slowest for polymers **1**, the rest of the elastomers were placed in between. After 32 days of incubation the PTX release was $11.5 \pm 0.8\%$, $15.3 \pm 2.3\%$, $18.4 \pm 1.6\%$ $23.8 \pm 3.4\%$,

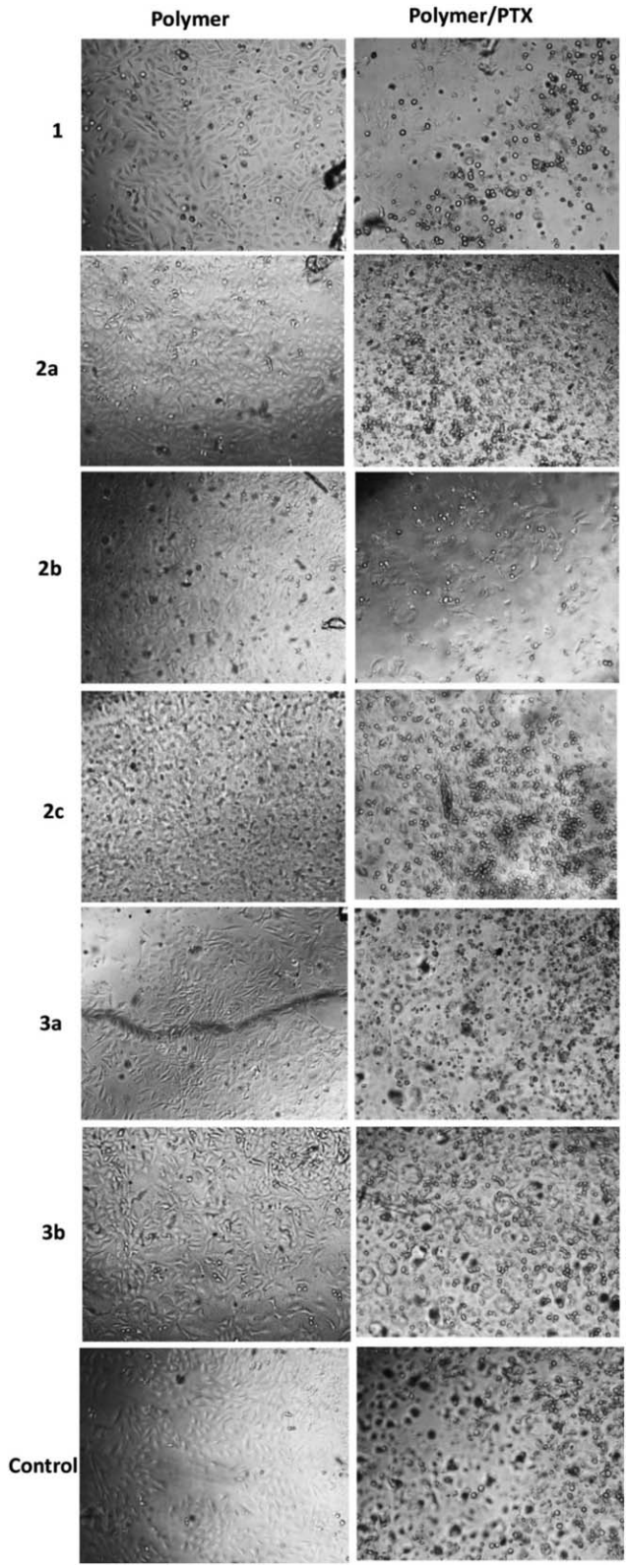

FIGURE 10 Phase contrast images of in vitro cell adhesion after 72 h of culturing A549 cells (×100 magnification).

58.9 ± 6.1%, and 76.0 ± 11.8% for polymers **1**, **2a**, **2b**,**3a, 3b**, and **2c**, respectively. The release rates follow the same trend as the mass loss over the degradation time. Moreover, from the evaluation of the amount (μg) of PTX released per day is evident the burst release is minimum when PTX loaded experiments were performed in THF [Fig. 8(c)]. Conversely, the polymers loaded in DCM showed a more pronounced initial burst phase, especially for elastomers **2c** and **3b** [Fig. 8(d)], which exhibited a maximum release of 17.03 ± 2.47 μg/day and 19.83 ± 2.47 μg/day during the first 7 day of incubation, which later stabilize to approximately 10 and 9 μg/day, for elastomers **2c** and **3b**, respectively.

In Vitro Anti-Tumor Activity

Adenocarcinomic human alveolar basal epithelial cells, (A549 line), was chosen as cell line model to evaluate the anti-proliferative effect on cancer cells.

Cells were seeded on each elastomer, which was previously placed on the bottom of the well. Cell proliferation was evaluated by MTS assay after 3, 5, and 7 days of exposure (Fig. 9).

During the first 72 h of exposure, proliferation of cancer cells was inhibited on all materials, with no significant difference on the absorbance between polymers and polymers loaded with PTX, with the exception of polymer **2c** (Fig. 9). However, after analyzing cell morphology through phase contrast images, it can be seen that cells seeded on the films loaded with PTX showed low viability in comparison with plain materials (Fig. 10); this tendency was observed during the whole time of exposure.

These interesting results support the hypothesis that elastomers containing PEG may act as cytostatic materials themselves, in agreement with published results.

Intriguingly, polymer **1**, which does not contain PEG, also has cytostatic effect, but to a lesser extent than polymers **2** and **3.**

PTX addition for local release showed a potent cytotoxic effect on all experiments. As shown by phase contrast images in Figure 10, after exposure, cells no longer showed an elongated morphology; instead cells look shrunk and rounded up, with a classic morphology of dead cells. Therefore, these results suggest that the combined cytostatic effect of the materials with the cytotoxic effect of PTX could be useful for controlling or/and inhibiting tumor growth.

CONCLUSIONS

A set of elastomers have been synthesized by a two-step polymerization technique and were fully characterized, showing easily tunable properties by selecting adequate curing conditions and monomers molar ratios.

THF was the most suitable solvent for loading PTX to the elastomers, as it did not compromise the mechanical properties of the film. PTX release tests proved to be sustained and constant for a long period of time. Anti-proliferative studies have shown that plain materials had cytostatic effects, preventing cancer cells to proliferate. Noteworthy, the addition of PTX for local site delivery resulted on low cell viability. Finally, these interesting new materials may find application for controlling tumor growth.

ACKNOWLEDGMENTS

This work was supported by Consejo Nacional de Investigaciones Científicas y Técnicas (CONICET) from Argentina. L. N. deeply acknowledges the postdoctoral fellowship received from CONICET.

REFERENCES AND NOTES

1 E. Mazza, A. E. Ehret, *J. Mech. Behav. Biomed. Mater.* **2015**, *48*, 100.

2 Q. Liu, L. Jiang, R. Shi, L. Zhang, *Prog. Polym. Sci.* **2012**, *37*, 715.

3 A. S. Xue, J. C. Koshy, W. M. Weathers, E. M. Wolfswinkel, Y. Kaufman, S. E. Sharabi, R. H. Brown, M. J. Hicks, L. H. Hollier Jr., *Craniomaxillofac. Trauma Reconstr.* **2014**, *7*, 27.

4 T. J. Webster, *Nanotechnology for the Regeneration of Hard and Soft Tissues*; World Scientific: Singapore, **2007**.

5 Q. Chen, S. Liang, G. A. Thouas, *Prog. Polym. Sci.* **2013**, *38*, 584.

6 S.L. Cooper, J. Guan, *Advances in Polyurethane Biomaterials*; Woodhead Publishing: Cambridge, England, **2016**.

7 J. Fromstein, K. Woodhouse, *J. Biomater. Sci. Polym. Ed.* **2002**, *13*, 391.

8 C. Martin-Mondiere, P. David, D. Loisance, *Ann. Vasc. Surg.* **1990**, *4*, 52.

9 I. Ali, N. Jamil, *Front. Biol.* **2016**, *11*, 19.

10 T. Zhang, B. A. Howell, A. Dumitrascu, S. J. Martin, P. B. Smith, *Polymer* **2014**, *55*, 5065.

11 L. Navarro, N. Ceaglio, I. Rintoul, *Polym. J.* **2017**, *49*, 625.

12 L. Navarro, D. E. Mogosanu, T. de Jong, A. D. Bakker, D. Schaubroeck, J. Luna, I. Rintoul, J. Vanfleteren, P. Dubruel, *Macromol. Biosci.* **2016**, *16*, 1678.

13 X. J. Loh, A. A. Karim, C. Owh, *J. Mater. Chem. B* **2015**, *3*, 7641.

14 R. Rai, M. Tallawi, A. Grigore, A. R. Boccaccini, *Prog. Polym. Sci.* **2012**, *37*, 1051.

15 J. P. Bruggeman, B.-J. de Bruin, C. J. Bettinger, R. Langer, *Biomaterials* **2008**, *29*, 4726.

16 Y. D. Wang, G. A. Ameer, B. J. Sheppard, R. Langer, *Nat. Biotechnol.* **2002**, *20*, 602.

17 Z. J. Sun, C. Chen, M. Z. Sun, C. H. Ai, X. L. Lu, Y. F. Zheng, B. F. Yang, D. L. Dong, *Biomaterials* **2009**, *30*, 5209.

18 Q.-Z. Chen, H. Ishii, G. A. Thouas, A. R. Lyon, J. S. Wright, J. J. Blaker, W. Chrzanowski, A. R. Boccaccini, N. N. Ali, J. C. Knowles, S. E. Harding, *Biomaterials* **2010**, *31*, 3885.

19 C. J. Bettinger, B. Orrick, A. Misra, R. Langer, J. T. Borenstein, *Biomaterials* **2006**, *27*, 2558.

20 I. Djordjevic, N. R. Choudhury, N. K. Dutta, S. Kumar, *Polym. Int.* **2011**, *60*, 333.

21 D. Gyawali, R. T. Tran, K. J. Guleserian, L. Tang, J. Yang, *J. Biomater. Sci. Polym. Ed.* **2010**, *21*, 1761.

22 J. Yang, A. R. Webb, S. J. Pickerill, G. Hageman, G. A. Ameer, *Biomaterials* **2006**, *27*, 1889.

23 J. P. Bruggeman, C. J. Bettinger, C. L. E. Nijst, D. S. Kohane, R. Langer, *Adv. Mater.* **2008**, *20*, 1922.

24 J. P. Bruggeman, C. J. Bettinger, R. Langer, *J. Biomed. Mater. Res. A* **2010**, *95*, 92.

25 D. G. Barrett, W. Luo, M. N. Yousaf, *Polym. Chem.* **2010**, *1*, 296.

26 H. R. Kricheldorf, G. Behnken, *Macromolecules* **2008**, *41*, 5651.

27 E. Harper, W. Dang, R. G. Lapidus, R. I. Garver, *Clin. Cancer Res.* **1999**, *5*, 4242.

28 T. Iwamoto, *Biol. Pharm. Bull.* **2013**, *36*, 715.

29 J. Hu, S. Fu, Q. Peng, Y. Han, J. Xie, N. Zan, Y. Chen, J. Fan, *Int. J. Pharm.* **2017**, *516*, 313.

30 J. Xu, L. Ma, Y. Liu, F. Xu, J. Nie, G. Ma, *Int. J. Biol. Macromol.* **2012**, *50*, 438.

31 R. Yang, S. G. Yang, W. S. Shim, F. Cui, G. Cheng, I. W. Kim, D. D. Kim, S. J. Chung, C. K. Shim, *J. Pharm. Sci.* **2009**, *98*, 970.

32 J. B. Wolinsky, Y. L. Colson, M. W. Grinstaff, *J. Controlled Release* **2012**, *159*, 14.

33 D. Naigamwalla, M. C. Chia, T. T. Tran, A. Medline, K. Hay, S. Gallinger, W. R. Bruce, *Cancer Res.* **2000**, *60*, 6856.

34 H. K. Roy, J. K. Di Baise, J. Black, W. J. Karolski, A. Ratashak, S. Ansari, *FEBS Lett.* **2001**, *496*, 143.

35 R. Z. Sangeda, J. Vandepitte, A. Huygens, B. Van Cleynenbreugel, H. Van Poppel, P. A. de Witte, *Anti-Cancer Drugs* **2010**, *21*, 645.

36 G. Parnaud, D. E. Corpet, L. Gamet-Payrastre, *Int. J. Cancer* **2001**, *92*, 63.

37 G. Liu, Y. Li, L. Yang, Y. Wei, X. Wang, Z. Wang, L. Tao, *RSC Adv.* **2017**, *7*, 18252.

38 A. F. Stalder, T. Melchior, M. Müller, D. Sage, T. Blu, M. Unser, *Colloids Surf. A* **2010**, *364*, 72.

39 M. González, S. E. Vaillard, *Curr. Org. Chem.* **2013**, *17*, 975.

40 T. D. Farahani, A. A. Entezami, H. Mobedi, *Iran. Polym. J.* **2005**, *14*, 753.